DALAT UNIVERSITY JOURNAL OF SCIENCE Volume 11, Issue 1, 2021 104-114

PLASMON MODES IN A MULTILAYER STRUCTURE WITH 3-BILAYER GRAPHENE SHEETS

Nguyen Van Men[a*], Dong Thi Kim Phuong[a], Vu Dong Duong[a]

[a]The Faculty of Education, An Giang University, Vietnam National University Ho Chi Minh City, An Giang, Vietnam
[*]Corresponding author: Email: nvmen@agu.edu.vn

Article history
Received: October 24th, 2020
Received in revised form: March 11th, 2021 | Accepted: March 13th, 2021
Available online: March 29th, 2021

Abstract

Recent research demonstrates that graphene has unique properties and applications in many technological fields. This paper presents results calculated within random phase approximation at zero temperature for collective excitations, an important characteristic of materials, in a three-layer structure consisting of three bilayer graphene sheets in an inhomogeneous background dielectric. Numerical calculations show that one optical and two acoustic branches exist in the system. The optical branch becomes overdamped quickly while the two acoustic branches continue and disappear at single-particle excitation boundaries. The increase in carrier density in the layers significantly decreases the frequencies of plasmon modes. The inhomogeneity of the background dielectric decreases the frequency of the higher branches but increases that of the lower branch. The effects of interlayer separation on plasmon modes are similar to those in homogeneous systems. Our results may provide more information and contribute to improving the theory of graphene.

Keywords: Bilayer graphene; Collective excitations; Inhomogeneous background dielectric; Three-layer structures.

DOI: http://dx.doi.org/10.37569/DalatUniversity.11.1.781(2021)

Article type: (peer-reviewed) Full-length research article

1. INTRODUCTION

In recent years, the distinct properties and technological applications of monolayer graphene (MLG) have become of much interest to scientists (Politano et al., 2017; Politano et al., 2016; Politano et al., 2018; Ryzhii et al., 2013a; Ryzhii et al., 2013b). Graphene has an excellent two-dimensional structure consisting of one layer of carbon atoms in which quasi-particles are considered massless fermions with linear dispersion and gapless energy. The density and mobility of carriers in graphene are much larger than those in recent semi-conductors. Moreover, the carrier density in graphene can be controlled easily by the electrostatic polarization method, although that method is impossible to apply for other materials. Because of these unique characteristics, graphene is considered a promising candidate for applications in a variety of technological fields (DasSarma et al., 2011; DasSarma et al., 2010; Geim & Novoselov, 2007; Maier, 2007; McCann, 2011). Bilayer graphene (BLG) is a structure consisting of two parallel MLG sheets separated by a small distance. The interactions between electrons in the two MLG sheets make quasi-particles in BLG become chiral massive fermions with parabolic low-energy dispersion. Hence, BLG and BLG-based structures have many interesting features compared to those of MLG and conventional two-dimensional electron gases (DasSarma et al., 2011; Sensarma et al., 2011).

Collective excitations in materials have been studied intensively and applied to create plasmonic devices for many years. It is known that collective excitations in graphene range from THz to infrared light, compared to visible light of plasmon in metals, so this material may be applied in this frequency region (Hwang & DasSarma, 2007; Sensarma et al., 2011). The reason is that quasi-particles in MLG behave as massless Dirac fermions with a gapless energy spectrum (Ryzhii & Ryzhii, 2007; Ryzhii et al., 2007). Recently, scientists have paid much attention to multilayer graphene systems. Their investigations show that plasmon properties in multilayer graphene systems have many interesting new features compared to those in monolayer systems. The frequency of optical and high-frequency acoustic modes increases, while the lowest-frequency acoustic mode decreases because of the interactions between electrons in multilayer graphene systems compared to plasmon in MLG (Hwang & DasSarma, 2009; Nguyen, 2020; Nguyen et al., 2019b; Dong & Nguyen, 2020; Vazifehshenas et al., 2010; Zhu et al., 2013). The background dielectric significantly affects the essential properties of layered structures. This factor directly affects Coulomb potentials between electrons in the system, and it also generates a small gap in the energy spectrum of MLG (Hwang & DasSarma, 2007; Nguyen et al., 2020; Nguyen & Dong, 2020; Patel et al., 2015b; Principi et al., 2012). Moreover, previous research has found that the inhomogeneity of the background dielectric in multilayer structures has noticeable effects on collective excitations (Badalyan & Peeters, 2012; Q. Nguyen & V. Nguyen, 2018; Dong & Nguyen, 2019). However, this factor is usually neglected because of the complicated calculations for the dynamical dielectric function of multilayer systems (Nguyen, 2020; Nguyen et al., 2019b; Zhu et al., 2013).

Scientists have introduced some useful methods to find solutions to many-body problems. The disturbance method provides good results in the first-order limit, but it

leads to divergent second-order solutions. The Green function method can also help find better solutions but with more complicated analytical calculations. The dielectric formalism is an effective method to investigate many-body systems and determine ground state energy, transport properties, and collective excitations by calculating the dynamical dielectric function. The dynamical dielectric function can be determined by certain approximations, depending on the characteristics of the system and the required accuracy of the results. It is well-known that random phase approximation is appropriate for high-density systems such as graphene (DasSarma et al., 2010; Nguyen, 2016). Collective excitations (plasmon) can be calculated from the poles of the pair-correlation function. However, it is proven from the Maxwell equations that plasma oscillations in the systems exist once the dynamical dielectric function equals zero. In other words, collective excitations in layered structures can be found from the zeroes of the dynamical dielectric function (Hwang & DasSarma, 2009; Patel et al., 2015a; Ta, 2017; Vazifehshenas et al., 2010). This paper presents calculations for collective excitations in a multilayer structure with 3-BLG sheets in an inhomogeneous background dielectric at zero temperature from the zeroes of the dynamical dielectric function within random phase approximation. The numerical results may provide useful information for technological applications of graphene.

2. THEORETICAL APPROACH

The model investigated in this paper, shown in Figure 1, consists of three parallel BLG sheets perpendicular to the Oz direction at $z = 0$, $z = d$, and $z = 2d$. The inhomogeneous background dielectric includes four layers with different dielectric constants κ_α $(\alpha = 1 \div 4)$. Each BLG sheet is doped homogeneously with carrier density n_i $(i = 1 \div 3)$, so the Fermi wave vector and the Fermi energy are uniform over the graphene lattice. Note that the BLG sheets in this paper are considered a two-dimensional structure with parabolic low-energy dispersion. In this approximation, the Hamiltonian of BLG has the form (DasSarma et al., 2010; Sensarma et al., 2011):

$$\widehat{H}_{2,xy} = -\frac{1}{2m}\begin{pmatrix} 0 & (k_x - ik_y)^2 \\ (k_x + ik_y)^2 & 0 \end{pmatrix} \tag{1}$$

in which $m = 0.033\, m_0$ is the effective mass, and m_0 is the vacuum mass of electrons. The energy and the wave function are:

$$E = \pm\frac{k^2}{2m}, \quad \psi_\pm = \frac{1}{\sqrt{2}}\begin{pmatrix} 0 \\ \mp e^{i2\varphi} \end{pmatrix} e^{i\vec{k}\vec{r}}\ . \tag{2}$$

The upper and the lower signs correspond to the conduction and the valence band, respectively, and φ is the argument of the wave vector in the graphene plane $\vec{k} = (k_x, k_y) = k(cos\,\varphi\,, sin\,\varphi)$.

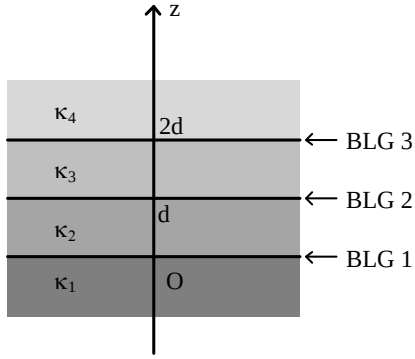

Figure 1. A 3-BLG structure in an inhomogeneous background dielectric

Collective excitations in the system can be determined from the zeroes of the dynamical dielectric function (V. Nguyen & Q. Nguyen, 2018; Nguyen et al., 2019a; Nguyen & Dong, 2019; Dinh & Nguyen, 2013; Vazifehshenas et al., 2010; Zhu et al., 2013):

$$\varepsilon\left(q, \omega_p - i\gamma\right) = 0. \tag{3}$$

Here, ω_p is the plasmon frequency at a given wave vector q, and γ is the damping rate of the respective plasma oscillations. In the case of weak damping, the solutions of Equation (3) can be found approximately from the solutions of the zeroes of the real part of the dielectric function (V. Nguyen & Q. Nguyen; Nguyen et al., 2019a; Nguyen & Dong, 2019; Dinh & Nguyen, 2013; Vazifehshenas et al., 2010; Zhu et al., 2013):

$$Re\,\varepsilon\left(q, \omega_p\right) = 0. \tag{4}$$

The damping rate can be calculated from the following equation:

$$\gamma = Im\,\varepsilon\left(q, \omega_p\right)\left(\frac{\partial\, Re\,\varepsilon(q,\omega)}{\partial\omega}\Big|_{\omega=\omega_p}\right)^{-1}. \tag{5}$$

The dynamical dielectric function of the system is given by (Nguyen, 2020; Nguyen et al., 2019b; Zhu et al., 2013):

$$\varepsilon(q, \omega) = det\left|1 - \hat{v}(q)\widehat{\Pi}(q, \omega)\right|. \tag{6}$$

where $\widehat{\Pi}(q, \omega)$ is the polarizability tensor of the system. As BLG sheets are isolated by sufficiently large separations, the electron tunneling between the BLG layers can be neglected. As a result, the non-diagonal elements of the polarizability tensor are set to zero, so we have:

$$\widehat{\Pi}(q, \omega) = \delta_{ij}\Pi_0^i(q, \omega) \tag{7}$$

where $\Pi_0^i(q,\omega)$ $(i = 1 \div 3)$ is the non-temperature polarizability function of BLG with parabolic low-energy dispersion observed by Sensarma and co-workers (Sensarma et al., 2011).

The Coulomb potential $\hat{v}(q)$ between carriers in BLG sheets can be found from the Poisson equation. The analytical expressions for the elements of this tensor are (Dong & Nguyen, 2019; Principi et al., 2012):

$$v_{ij}(q) = \frac{2\pi e^2}{q} f_{ij}(q). \tag{8}$$

In Equation (8), $f_{ij}(x)$ $(i,j = 1 \div 3)$ are:

$$f_{11}(q) = \frac{2\left[(\kappa_2+\kappa_3)(\kappa_3-\kappa_4)+2\kappa_3(\kappa_2-\kappa_3)e^{2qd}+(\kappa_2+\kappa_3)(\kappa_3+\kappa_4)e^{4qd}\right]}{M(qd)}, \tag{9}$$

$$f_{22}(q) = \frac{8e^{2qd}[\kappa_1\, cosh(qd)+\kappa_2\, sinh(qd)][\kappa_3\, cosh(qd)+\kappa_4\, sinh(qd)]}{M(qd)}, \tag{10}$$

$$f_{33}(q) = \frac{2\left[(\kappa_2+\kappa_3)(\kappa_2-\kappa_1)+2\kappa_2(\kappa_3-\kappa_2)e^{2qd}+(\kappa_1+\kappa_2)(\kappa_2+\kappa_3)e^{4qd}\right]}{M(qd)}, \tag{11}$$

$$f_{12}(q) = f_{21}(q) = \frac{8\kappa_2 e^{2qd}[\kappa_3\, cosh(qd)+\kappa_4\, sinh(qd)]}{M(qd)}, \tag{12}$$

$$f_{13}(q) = f_{31}(q) = \frac{8\kappa_2\kappa_3 e^{2qd}}{M(qd)}, \tag{13}$$

$$f_{32}(q) = f_{23}(q) = \frac{8\kappa_3 e^{2qd}[\kappa_2\, cosh(qd)+\kappa_1\, sinh(qd)]}{M(qd)}, \tag{14}$$

with

$$\begin{aligned} M(x) = {} & (\kappa_1-\kappa_2)(\kappa_2+\kappa_3)(\kappa_3-\kappa_4) + 2e^{2x}(\kappa_2-\kappa_3)(\kappa_1\kappa_3-\kappa_2\kappa_4) \\ & + e^{4x}(\kappa_1+\kappa_2)(\kappa_2+\kappa_3)(\kappa_3+\kappa_4). \end{aligned} \tag{15}$$

The expressions for $f_{ij}(x)$ show the pronounced dependence of the Coulomb potentials on the inhomogeneity of the background dielectric. Obviously, the dynamical dielectric function and collective excitations are also affected remarkably by this factor. Therefore, investigations of collective excitations, taking into account the inhomogeneity of the background dielectric, may be necessary to improve the model. By replacing the dynamical dielectric function in Equation (6) with the polarizability in Equation (7) and putting the Coulomb potentials of Equations (8-15) into Equation (4), we can determine collective excitations in the system. The solutions of Equation (4) are found by the half-distance method and are utilized to calculate the damping rate in Equation (5). The numerical results are presented in the following section.

3. NUMERICAL RESULTS AND DISCUSSION

Numerical calculations for collective excitations and the damping rate in the 3-BLG system in an inhomogeneous background dielectric, shown in Figure 1, are presented in this section. In the calculations, dielectric layers SiO_2 ($\kappa_1 = \kappa_{SiO_2} = 3.8$), BN ($\kappa_2 = \kappa_{BN} = 5.0$), hBN ($\kappa_3 = \kappa_{hBN} = 3.0$) and air ($\kappa_4 = \kappa_{air} = 1.0$) are used (Hwang & DasSarma, 2007, 2009; Svintsov et al., 2013). Note that k_F and E_F denote the Fermi wave vector and the Fermi energy of the first BLG sheet, respectively.

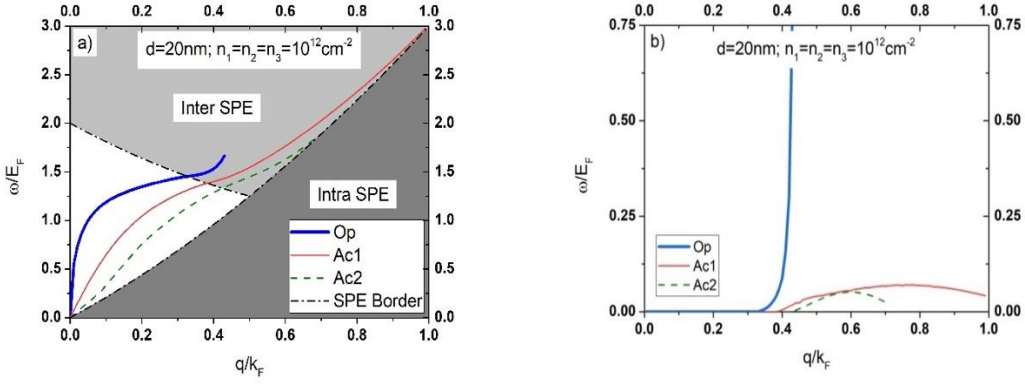

(a) (b)

Figure 2. Plasmon modes (a) and the damping rate (b) in a 3-BLG system, plotted for $d = 20\ nm$ and $n_1 = n_2 = n_3 = 10^{12}\ cm^{-2}$

Note: The dash-dotted lines show single-particle excitation (SPE) boundaries.

Figure 2 demonstrates collective excitations (a) and the damping rate (b) in a 3-BLG system with an inhomogeneous background dielectric. Following previous publications, the figure is plotted for $d = 20\ nm$, $n_1 = n_2 = n_3 = 10^{12}\ cm^{-2}$(Badalyan & Peeters, 2012; DasSarma et al., 2011; DasSarma et al., 2010; Hwang & DasSarma, 2009; Sensarma et al., 2011; Zhu et al., 2013). Numerical calculations show that Equation (4) admits three solutions, corresponding to three plasmon modes in the system, similar to those in other 3-layer structures (Nguyen, 2020; Nguyen et al., 2019b; Dong & Nguyen, 2019; Zhu et al., 2013). The optical branch (Op), which takes the highest frequency, crosses the boundary of inter single-particle excitation (SPE) then disappears at about $q = 0.45k_F$. The two acoustic plasmon branches (Ac), which take lower frequencies, continue until approaching the intra SPE boundary. This behavior of the Ac branches is similar to that in BLG observed by Sensarma's group (Sensarma et al., 2011). For further discussion, we note some observations on collective excitations of multilayer BLG structures from previous publications. In the case of double bilayer graphene (Nguyen et al., 2019a), the lower plasmon branch admits the SPE boundary and disappears while the higher branch becomes overdamped and loses its energy quickly. In the MLG-BLG double-layer structure, a similar phenomenon is found for the lower branch, but the higher branch, sharing the same feature with plasmon in MLG (Hwang & DasSarma, 2007), continues in the SPE region (Q. Nguyen & V. Nguyen, 2018). In the case of 3-layer structures with one BLG sheet, the lowest branch is damped strongly while

the others exist in larger wave vector areas. In 3-layer graphene systems with two BLG sheets, the highest branch continues in the SPE region while the lowest branch merges with the SPE boundary and the middle branch becomes overdamped and disappears (Dong & Nguyen, 2019). The similarity between the plasmon characteristics in the systems mentioned above is that the plasmon branches approach the SPE boundary or become overdamped in the case of BLG (Nguyen et al., 2019a; Sensarma et al., 2011) while the branch continues in the SPE region in the other case (Hwang & DasSarma, 2007, 2009). With carrier density $n = 10^{12}\, cm^{-2}$, the Fermi energy of MLG (approximately 0.117 eV) is larger than that of BLG (about 0.036 eV), so the lower plasmon branch behaves similarly to that of BLG (Q. Nguyen & V. Nguyen, 2018; Dong & Nguyen, 2019). In this paper, we consider a system consisting of three BLG sheets; thus, collective excitations have features similar to that of BLG. This means that the largest energy branch (Op) becomes overdamped while the others touch the SPE boundary. The damping rate of the two Ac modes has a similar pattern, as seen in Figure 2b. However, the Op mode loses its energy quickly, so its damping rate increases strongly with the increase in wave vector, as seen in Figure 2b (thick solid line).

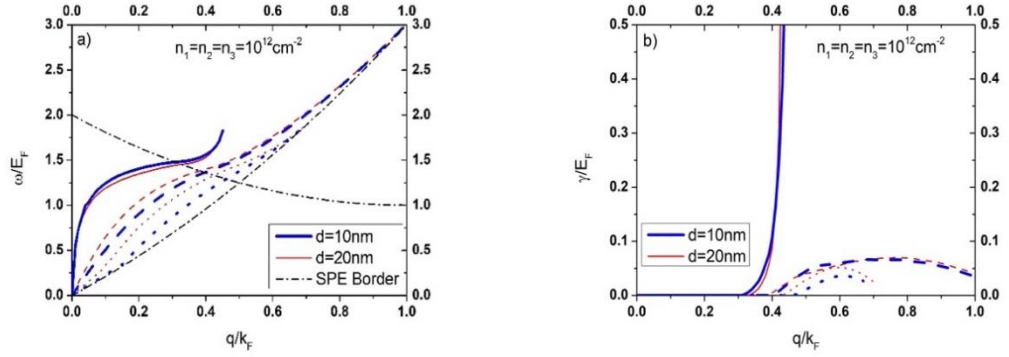

(a) (b)

Figure 3. Plasmon modes (a) and the damping rate (b) in a 3-BLG system with several interlayer distances, plotted for $n_1 = n_2 = n_3 = 10^{12}\, cm^{-2}$, $d = 10\, nm$ and $d = 20\, nm$

Note: Dash-dotted lines show SPE boundaries.

The dependence of collective excitations and respective damping rate in a 3-BLG system on interlayer distance is plotted in Figure 3 for $n_1 = n_2 = n_3 = 10^{12}\, cm^{-2}$. Figure 3a shows that the increase in interlayer distance decreases (increases) slightly (significantly) Op (Ac) plasmon frequency. However, both the pattern and the energy loss of plasmon branches depend weakly on separation. As seen in Figure 3b, Op modes are damped at $q \approx 0.3k_F$ while Ac modes lose their energy at about $q \approx 0.4k_F \div 0.45k_F$ for both separations $d = 10\, nm$ and $d = 20\, nm$.

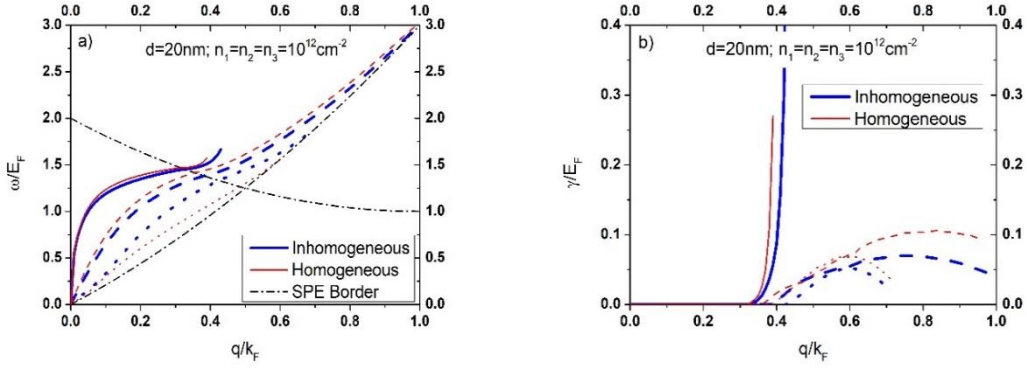

(a) (b)

Figure 4. Plasmon frequency (a) and respective damping rate (b) in homogeneous and inhomogeneous 3-BLG systems

Note: Dash-dotted lines show SPE boundaries.

Now we turn to study the effects of the inhomogeneity of the background dielectric on plasmon properties in 3-BLG systems. Figure 4 plots plasmon modes and the decay rate of plasma oscillations in a 3-BLG system with a homogeneous and inhomogeneous background dielectric for the same carrier density and interlayer distance. In the case of the homogeneous system, the average permittivity $\bar{\kappa} = (\kappa_1 + \kappa_4)/2 = 2.4$ is used (Badalyan & Peeters, 2012). The figure demonstrates that the inhomogeneity of the background dielectric strongly affects plasmon modes. The frequencies of Op and Ac1 in the case of the homogeneous system are smaller than those of the other case. By contrast, the frequency of the Ac2 mode in the homogeneous system is much smaller than that in the inhomogeneous system. This behavior differs sharply from that in the double bilayer graphene structure observed previously (Nguyen et al., 2019a). Figure 4b shows that the decay rate of plasma oscillations in the inhomogeneous system has smaller values compared to that in the homogeneous system at a given wave vector.

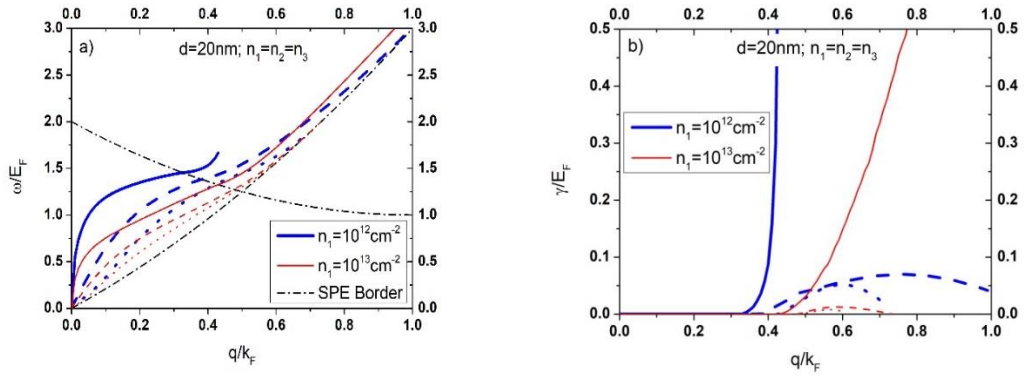

(a) (b)

Figure 5. Plasmon modes (a) and the damping rate (b) in a 3-BLG system for several carrier densities

Note: Dash-dotted lines show SPE boundaries.

Finally, to investigate the effects of the doping density on the collective excitations and damping rate, Figure 5 presents plasmon modes (a) and the damping rate (b) in a 3-BLG system with two doping densities, $n = 10^{12}\ cm^{-2}$ and $n = 10^{13}\ cm^{-2}$. It can be seen from Figure 5a that in the case of carrier density $n = 10^{13}\ cm^{-2}$, the frequencies of three plasmon branches are much lower than the respective frequencies in the other case, $n = 10^{12}\ cm^{-2}$. Moreover, in the case of the larger carrier density, although the Op mode is damped, this mode continues in SPE, so the damping rate increases more slowly than in the lower carrier density case, as seen in Figure 5b.

4. CONCLUSION

In summary, collective excitations are calculated for the first time for a multilayer structure with 3-BLG in an inhomogeneous background dielectric at zero temperature. The numerical calculations show that three plasmon modes exist in the system, similar to those in other three-layer structures. The optical mode only exists in the small wave vector region because this mode is damped strongly after crossing the SPE boundary. On the other hand, two acoustic modes continue and only disappear on approaching the SPE boundary, similar to plasmon in BLG. The investigations on collective excitations illustrate that the increase in interlayer distance decreases (increases) the frequency of Op (Ac) branch(es) while the inhomogeneity of the background dielectric decreases the frequencies of the two higher branches but increases the frequency of the lowest one. Finally, the increase in doping density remarkably decreases plasmon frequencies in the systems.

ACKNOWLEDGMENT

This research is funded by Vietnam National University Ho Chi Minh City (VNU-HCM) under grant number C2021-16-06.

REFERENCES

Badalyan, S. M., & Peeters, F. M. (2012). Effect of nonhomogenous dielectric background on the plasmon modes in graphene double-layer structures at finite temperatures. *Physical Review B, 85*(19), 195444.

DasSarma, S., Adam, S., Hwang, E. H., & Rossi, E. (2011). Electronic transport in two dimensional graphene. *Reviews of Modern Physics, 83*, 407-470.

DasSarma, S., Hwang, E. H., & Rossi, E. (2010). Theory of carrier transport in bilayer graphene. *Physical Review B, 81*, 161407.

Dong, T. K. P., & Nguyen, V. M. (2019). Plasmon modes in 3-layer graphene structures: Inhomogeneity effects. *Physics Letters A, 383*, 125971.

Dong, T. K. P., & Nguyen, V. M. (2020). Plasmon modes in N-layer graphene structures at zero temperature. *Journal of Low Temperature Physics, 201*, 311-320.

Dinh, V. T., & Nguyen, Q. K. (2013). Plasmon modes of double-layer graphene at finite temperature. *Physica E, 54*, 267-272.

Geim, A. K., & Novoselov, K. S. (2007). The rise of graphene. *Nature Materials, 6*, 183-191.

Hwang, E. H., & DasSarma, S. (2007). Dielectric function, screening, and plasmons in two-dimensional graphene. *Physical Review B, 75*, 205418.

Hwang, E. H., & DasSarma, S. (2009). Exotic plasmon modes of double layer graphene. *Physical Review B, 80*, 205405.

Maier, S. A. (2007). *Plasmonics: Fundamentals and applications*. Springer.

McCann, E. (2011). Electronic properties of monolayer and bilayer graphene. In H. Raza (Ed.) *Graphene nanoelectronics* (pp. 237-275). Springer.

Nguyen, Q. K. (Ed.). (2016). *Theory of many-body system*. Vietnam National University Ho Chi Minh City.

Nguyen, Q. K. & Nguyen, V. M. (2018). Plasmon modes in bilayer-monolayer graphene heterostructures. *Physica Status Solidi B, 255*(7), 1700656.

Nguyen, Q. K. & Nguyen, V. M. (2018). Plasmon modes in Dirac-Schrödinger hybrid electron systems including layer-thickness and exchange-correlation effects. *Canadian Journal of Physics, 96*, 615-621.

Nguyen, Q. K., Nguyen, V. M., & Dong, T. K. P. (2019a). Plasmon modes in double bilayer graphene heterostructures. *Solid State Communications, 294*, 43-48.

Nguyen, Q. K., Nguyen, V. M., & Dong, T. K. P. (2019b). Plasmon modes in N-layer bilayer graphene structures. *Solid State Communications, 298*, 113647.

Nguyen, Q. K., Nguyen, V. M., & Dong, T. K. P. (2020). Plasmon modes in double-layer gapped graphene. *Physica E, 118*, 113859.

Nguyen, V. M. (2020). Plasmon modes in N-layer gapped graphene. *Physica B, 578*, 411876.

Nguyen, V. M., & Dong, T. K. P. (2019). Plasmon modes in graphene GaAs heterostructures at finite temperature. *International Journal of Modern Physics B, 33*(16), 1950174.

Nguyen, V. M., & Dong, T. K. P. (2020). Plasmon modes in double-layer gapped graphene at zero temperature. *Physics Letters A, 384*, 126221.

Patel, D. K., Ashraf, S. S. Z., & Sharma, A. C. (2015a). Finite temperature dynamical polarization and plasmons in gapped graphene. *Physica Status Solidi B, 252*(8), 1817-1826.

Patel, D. K., Ashraf, S. S. Z., & Sharma, A. C. (2015b). Temperature dependent screened electronic transport in gapped graphene. *Physica Status Solidi B, 252*(2), 282-287.

Politano, A., Chiarello, G., & Spinella, C. (2017). Plasmon spectroscopy of graphene and other two-dimensional materials with transmission electron microscopy. *Materials Science in Semiconductor Processing, 65*, 88-99.

Politano, A., Cupolillo, A., Profio, G. D., Arafat, H. A., Chiarello, G., & Curcio, E. (2016). When plasmonics meets membrane Technology. *Journal of Condensed Matter Physics, 28*, 363003.

Politano, A., Yu, H. K., Farías, D., & Chiarello, G. (2018). Multiple acoustic surface plasmons in graphene/Cu(111) contacts. *Physical Review B, 97*, 035414.

Principi, A., Carrega, M., Asgari, R., Pellegrini, V., & Polini, M. (2012). Plasmons and Coulomb drag in Dirac/Schroedinger hybrid electron systems. *Physical Review B, 86*, 085421.

Ryzhii, V., & Ryzhii, M. (2007). Negative dynamic conductivity of graphene with optical pumping. *Journal of Applied Physics, 101*, 083114.

Ryzhii, V., Ryzhii, M., Mitin, V., Shur, M. S., Satou, A., & Otsuji, T. (2013a). Injection terahertz laser using the resonant inter-layer radiative transitions in double-graphene-layer structure. *Journal of Applied Physics, 103*, 163507.

Ryzhii, V., Ryzhii, M., Mitin, V., Shur, M. S., Satou, A., & Otsuji, T. (2013b). Terahertz photomixing using plasma resonances in double-graphene layer structures. *Journal of Applied Physics, 113*, 174506.

Ryzhii, V., Satou, A., & Otsuji, T. (2007). Plasma waves in two-dimensional electron-hole system in gated graphene heterostructures. *Journal of Applied Physics, 101*, 024509.

Sensarma, R., Hwang, E. H., & DasSarma, S. (2011). Dynamic screening and low energy collective modes in bilayer graphene. *Physical Review B, 82*, 195428.

Svintsov, D., Vyurkov, V., Ryzhii, V., & Otsuji, T. (2013). Voltage-controlled surfaceplasmon-polaritons in double graphene layer structures. *Journal of Applied Physics, 113*, 053701.

Ta, H. S. (2017). *Plasmon characteristics and dynamical properties of electrons in graphene.* (Doctoral dissertation, Hanoi University of Science and Technology, Vietnam).

Vazifehshenas, T., Amlaki, T., Farmanbar, M., & Parhizgar, F. (2010). Temperature effect on plasmon dispersions in double-layer graphene systems. *Physics Letters A, 374*(48), 4899-4903.

Zhu, J.-J., Badalyan, S. M., & Peeters, F. M. (2013). Plasmonic excitations in Coulomb-coupled N-layer graphene structures. *Physical Review B, 87*, 085401.